Available online at www.sciencedirect.com
ScienceDirect
Journal of Photochemistry and Photobiology A: Chemistry 186 (2007) 115–120
Journal of Photochemistry and Photobiology A:Chemistry
www.elsevier.com/locate/jphotochem

Comparison of photooxidation and photoreduction reactions on TiO_2 nanoparticles

Terry A. Egerton *, John A. Mattinson

School of Chemical Engineering and Advanced Materials, Bedson Building, University of Newcastle Upon Tyne, Newcastle NE1 7RU, UK

Received 10 May 2006; received in revised form 25 July 2006; accepted 29 July 2006
Available online 5 August 2006

Abstract

Photooxidation and photoreduction reaction rates on nanoparticulate TiO_2 have been studied using a series of silica coated samples prepared from the same parent material—a high area rutile. Oxidation of propan-2-ol was measured by GC analysis of acetone product. Reduction of DPPH (1,1-diphenyl-2-picrylhydrazyl radical) was followed by the decrease in absorbance at 520 nm and photogreying of TiO_2 was measured as a change in L, the reflectance of the CIE Y illuminant centred at 550 nm, using a Minolta chroma meter.

The activity for oxidation of propan-2-ol correlated well with two measures of photoreduction, the reduction of the stable DPPH and TiO_2 photogreying in an oxygen free system.

In all cases, low silica loadings resulted in a small increase in activity. For silica levels >1 wt.% the dependence of activity decreased with increasing levels of silica treatment. The pattern of activity versus silica-level was consistent with elimination of both photooxidation and photoreduction at 12–16% silica. A speculative interpretation of these changes was based on changes in the silica environment as determined by magic angle spinning NMR.

Keywords: Photocatalysis; TiO_2 rutile; Potogreying; Propan-2-ol; DPPH

1. Introduction

TiO_2 photocatalysis has developed rapidly since early observations by, for example Stone [1,2]. Photoexcitation of rutile TiO_2 ($\lambda < 400$ nm) generates highly oxidising holes in the valence band (+2.7 V versus NHE at pH 7) and mildly reducing electrons in the conduction band (−0.5 V versus NHE). Photooxidation has been considered extensively by many authors, a wide range of molecules including alcohols [3–5], carboxylic acids [6–9] and substituted aromatics [10,11] have been studied in depth, and the mechanism of oxidation is generally understood. However, much less research has been done on photoreduction reactions (perhaps because the photogenerated electron is not particularly reducing).

The reduction of methyl-viologen ($MV^{2+}/MV^{\bullet+}$, $E^0 = -0.42$ (versus SHE)) has been studied [12,13] by monitoring the formation of the 602 nm absorption of the reduced molecule. The photocatalytic degradation of CCl_4 has also been shown to follow a reductive mechanism [14,15]. The details of this reaction are more complicated than methyl-viologen; oxygen does not have to be excluded from the system but does have an effect on the measured rate. In a separate study, Pelizzetti et al. [16] has shown that for a series of chloromethanes the importance of reduction decreases as the degree of substitution decreases, and dichloromethane degradation is essentially oxidative.

Truscott et al. [17] showed that the rate of TiO_2 photocatalysed bleaching of the DPPH absorption at 520 nm depended on the type of TiO_2, and followed the order P25 (uncoated, mainly anatase) > Tayca MT100T (coated rutile) > Ishihara FPT4-12 (coated rutile) ≥ Tayca MT100Z (coated rutile) > no TiO_2. Although the reaction of DPPH with solvated electrons, generated by pulse radiolysis, was very fast, with a rate constant of $1 \times 10^{10}\ M^{-1}\ s^{-1}$, bleaching during irradiation of Tayca MT100T followed a bi-exponential decay with rate constants of 5 and $0.6\ s^{-1}$ (speculated to be bi-exponential because the particle size of the TiO_2 exerted a controlling influence). They showed that neither water nor propan-2-ol affected the observed kinetics and that there was no significant difference in the rate

* Corresponding author. Tel.: +44 191 222 5618.
E-mail address: T.A.Egerton@ncl.ac.uk (T.A. Egerton).

1010-6030/$ – see front matter © 2006 Elsevier B.V. All rights reserved.
doi:10.1016/j.jphotochem.2006.07.018

Table 1
List of samples used for all experiments

Sample name	Surface treatment (wt.% SiO_2)	XRF analysis (wt.% SiO_2)
A	None	–
B	0.1	–
C	0.25	–
D	0.5	0.7
E	1	
F	3	3.2
G	5	
H	10	9.1

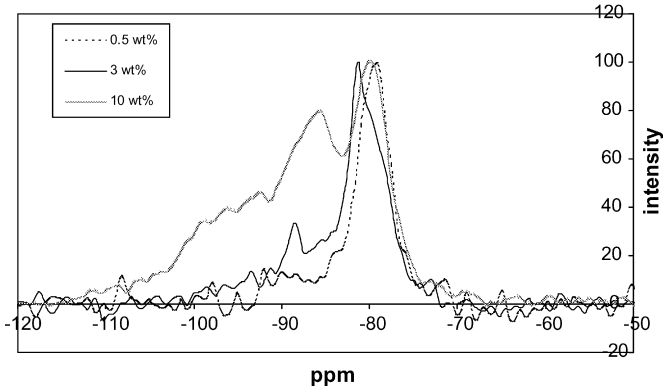

Fig. 1. Si-29 MAS NMR of three silica-TiO_2 samples, with silica loadings from 0.5 to 10 wt.%, measured using Varian Unity Inova spectrometer.

of decay when oxygen was replaced by argon. Although this study established mechanistic detail of the observed bleaching, no attempt was made to quantitatively compare the changes in the rate of reduction with other measures (e.g., propan-2-ol oxidation and photogreying) of photoactivity. Work by Wakefield et al. [18] has also utilised the DPPH reduction reaction for comparing a range of doped and coated rutile samples. In this case, the work was conducted in the dark in order to compare the intrinsic radical scavenging ability of the powders but not their photoactivity.

In this paper, we have examined in more detail the reduction of DPPH by a range of TiO_2 samples. To obtain a series of samples with different photoactivity but with no change in the primary particle size we have reduced the activity of a high area rutile sample by progressively covering the surface with silica. The effect of the silica coating on photoactivity has been determined by oxidation of propan-2-ol and the activity for photooxidation correlated with the activity for photoreduction of DPPH. We also report the correlation between the photoreduction of DPPH and the UV-induced photogreying of the TiO_2 samples. From this we conclude that photogreying is caused by the reduction of the TiO_2 (probably Ti^{4+} to Ti^{3+}) during UV irradiation in the absence of oxygen.

2. Experimental

2.1. Sample preparation

The materials used in this study are listed in Table 1. Sample A is high area (~140 $m^2\,g^{-1}$) rutile prepared by the hydrolysis of $TiCl_4$ and supplied by Uniqema. Samples B–H were all prepared from sample A.

All silica coatings were applied using Iler's "dense silica" method [19]. A 30 g dm^{-3} aqueous supension of sample A was heated to 90 °C at pH 9. To this, the required amount of sodium silicate was co-added (as an aqueous solution) with sulphuric acid to maintain a pH of 9. Once addition was complete the pH was adjusted to 6.5 and the slurry was filtered, washed and dried (110 °C for 16 h).

2.2. Sample characterisation

XRF confirmed that silica had been deposited. Deposition was successful at low, medium and high silica loadings. Solid state ^{29}Si magic angle spinning (MAS) NMR spectra were measured on three samples (0.5, 3.0 and 10.0 wt.%). The results confirmed the existence of silica on the surface but also gave more information about the environment of the silicon atoms in each case. The ^{29}Si NMR are given in Fig. 1 and show that the silicon are largely in Q^1 [O_3SiOSi] and Q^2 [$O_2Si(OSi)_2$] environments where there is a small amount of cross-linking [20]. At lower loadings a single peak was observed at −79 ppm which indicates only Q^1 type silica being present (and possibly Q^0) and negligible cross-linking. For the high silica content sample (10 wt.%) the spectrum showed a greater amount of Q^2 silicon was present as well as considerable Q^3 [$O_3Si(OSi)_3$] and potentially some Q^4 [$Si(OSi)_4$] bonding. This means that at higher loadings there is more of the condensed silica species than at lower loadings.

A numerical simulation based on the random occupation of a 400 × 400 square grid suggested that at low surface coverages (0.5 wt.%) 100% of the silica was present as Q^0 and Q^1, whereas at higher coverages (10 wt.%) approximately 95% of the silica was present as Q^2 and Q^3.

2.3. Photoactivity measurements

2.3.1. Propan-2-ol photooxidation

Oxidation of propan-2-ol was monitored by following the formation of acetone over time by gas chromatography (GC), as detailed elsewhere [21].

2.3.2. DPPH photoreduction

DPPH photoreduction was carried out in the same cell as used for propan-2-ol oxidation using the general method described by Truscott et al. [17]. The TiO_2 was dispersed in a solution of DPPH (Aldrich, 90%) in a 50:50 mix of mineral oil and caprylic acid triglyceride (MOTG; supplied by Uniqema). DPPH solutions were prepared fresh and used within 2–3 days of preparation. No degradation of DPPH (as determined by the initial UV–vis peak at 520 nm) was observed in this time period. The dependence of DPPH reduction rate on TiO_2 loading was investigated (Fig. 2) and showed no sign of a plateau. The final reaction mixture consisted of 50 cm^3 of 2×10^{-4} M DPPH with a standard TiO_2 concentration of 0.25 g dm^{-3}. The light source, as

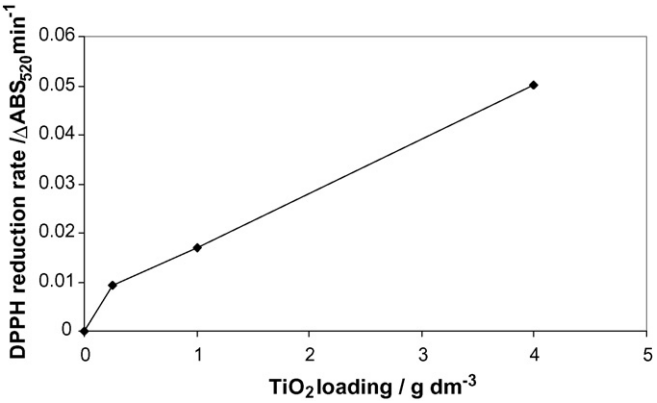

Fig. 2. Loading curve for DPPH• reduction reaction.

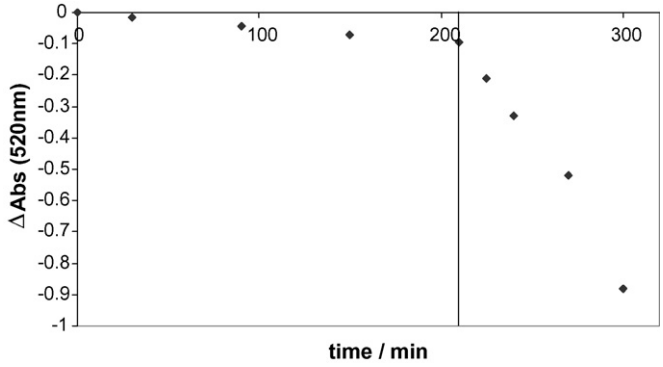

Fig. 4. Loss of peak at 520 nm without UV light (left of line) and with UV light (right of line) for a typical experiment in the presence of 0.25 g dm^{-3} TiO_2.

used for propan-2-ol oxidation [21] showed a maximum UV emission at 365 nm. Preliminary experiments showed that, at this loading level, the repeatability of replicate measurements was good, whereas at higher (8 g dm^{-3}) TiO_2 loadings, as used for propan-2-ol oxidation, the reaction was too fast to achieve consistent results. The mixture was stirred for 1 min before irradiation and 1 cm^3 of sample was removed at regular intervals and passed through a filter to remove the TiO_2 so that the UV–vis spectrum could be recorded using a Shimadzu UV-Mini 1240 spectrometer. The decrease of the peak at 520 nm represents the reduction of DPPH with the product absorbing very little in this region (Fig. 3). Wakefield has shown previously that there is a "dark" reaction associated with DPPH reduction [18]. For our system (Fig. 4) this "dark" reaction, to which adsorption could also contribute, was ca. twenty times slower than the UV reaction and was neglected in any results. In a typical experiment, the 520 nm peak fell from 1.5 to a minimum of 0.4 and plots of absorbance versus time were linear ($R^2 > 0.98$), but no attempt was made to establish kinetics of bleaching.

2.3.3. Photogreying measurements (ΔL)

The dispersions used for the photogreying experiments contained 5 wt.% of TiO_2 sample in a C_{12}–C_{15} alkyl benzoate (Finsolv) medium. The dispersions were prepared by milling the mixtures for 15 min at 5000 rpm with a "MINI MOTOR" mill (Eiger Torrance MK M50 VSE TFV), which was filled (70%) with zirconia beads (0.8–1.25 mm). The dispersions were then transferred to a reaction cell and placed on a turntable 12 cm beneath a 75 W UV light source. The quartz cover on the reaction cell is intended to maintain an oxygen free environment as oxygen would reverse/prevent the photogreying process. The quartz was held in place by a movable brass catch. Measurements of L, derived from the reflectance of the CIE Y illuminant with a maximum intensity at ~550 nm, were taken every 30 min for 240 min using a Minolta chroma meter (CR-300), previously calibrated against a white tile ($L = 97.95$). Egerton et al. have given elsewhere [22] a more detailed explanation of photogreying and its measurement.

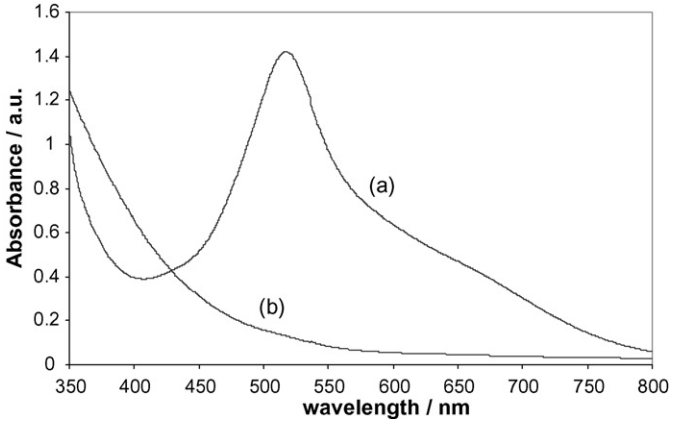

Fig. 3. DPPH• absorption spectra, 2×10^{-4} M, 0.5 cm path length (a) and $DPPH_2$ absorption (b).

3. Results

Photooxidation of propan-2-ol to propanone increased linearly with time, as previously reported [21]. For a series of silica-coated samples, a linear decrease in propan-2-ol oxidation rate was observed as silica loading was increased (Fig. 5a). Extrapolating the activity versus loading line suggests that a loading level of ~12 wt.% would be required to eliminate essentially all activity for propan-2-ol oxidation. This is in good agreement with the range of 9–20 wt.% reported by Egerton and Tooley [21] for a different series of samples prepared by silica coating a separate batch of TiO_2 similar, but not identical to A.

The DPPH 520 nm absorbance peak decreased linearly with time over the course of reaction studied here (Fig. 4). For TiO_2 samples with a higher level of silica coating the bleaching was slower and a corresponding analysis to that described above for propan-2-ol shows (Fig. 5b) that 16 wt.% silica would be required to remove all the bleaching ability of TiO_2. This value also falls within the range suggested previously.

Fig. 6 shows typical results for increased photogreying as a function of time. Comparisons between the photogreying of different samples were based on ΔL_{120}, photogreying after 120 min, when the values of L are no longer changing rapidly. If other ΔL values were used (90 or 150 min) the overall trend was essentially the same. Higher silica levels resulted in a decrease in photogreying (ΔL was less). Extrapolation of photogreying results versus % of silica content (Fig. 5b), as for the two

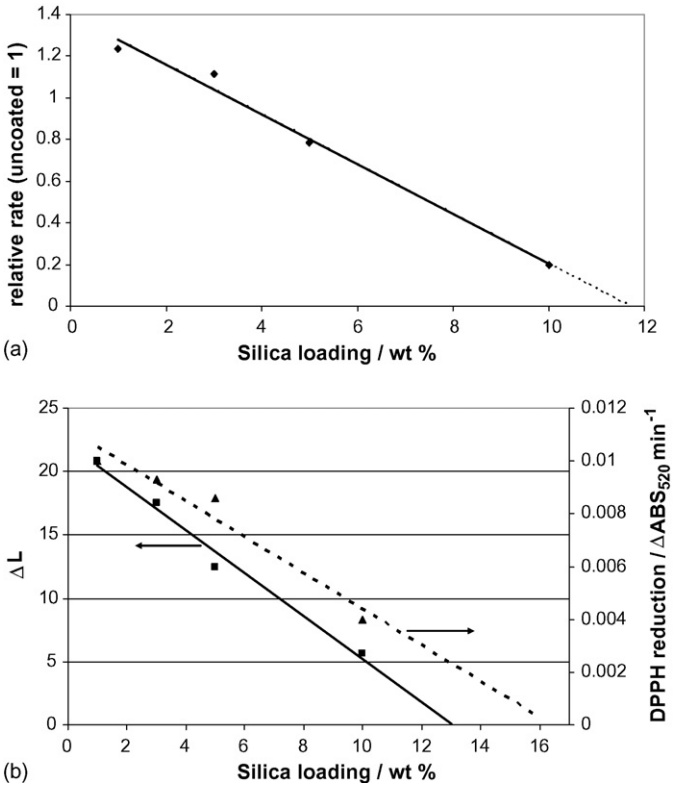

Fig. 5. (a) Decrease in relative propan-2-ol oxidation rate at higher silica coatings. The uncoated rutile has a relative rate of 1 (=9.33×10^{-5} mol dm^{-3} min^{-1}) and (b) linear decrease in rates of DPPH$^{\bullet}$ reduction (dashed line) and photogreying at 120 min (full line) at higher silica levels.

previous reactions, indicates that a coating level of 13 wt.% silica would reduce the amount of photogreying to a level close to 0.

Fig. 7 compares the measured photogreying at three different exposure times (for clarity five photogreying units were added to the 90 min values and five were subtracted from the 150 min values) with the rate of propan-2-ol photooxidation. Fig. 8 shows the corresponding comparison of the rates of DPPH photoreduction and propan-2-ol photooxidation. Both show a good correlation ($R^2 = 0.96$ for the former and 0.94 for the latter). Consequently a good correlation was also observed between photoreduction and photogreying measurements (Fig. 9).

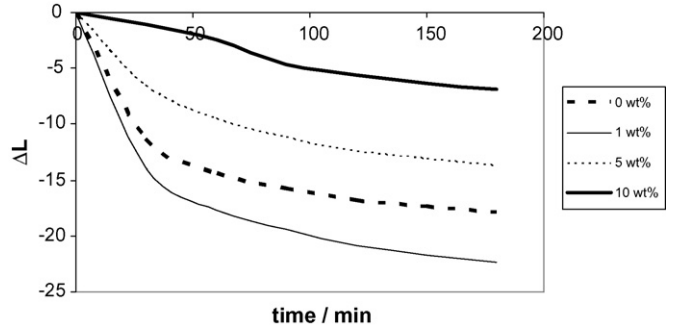

Fig. 6. Change in photogreying (ΔL) over time for a selection of samples.

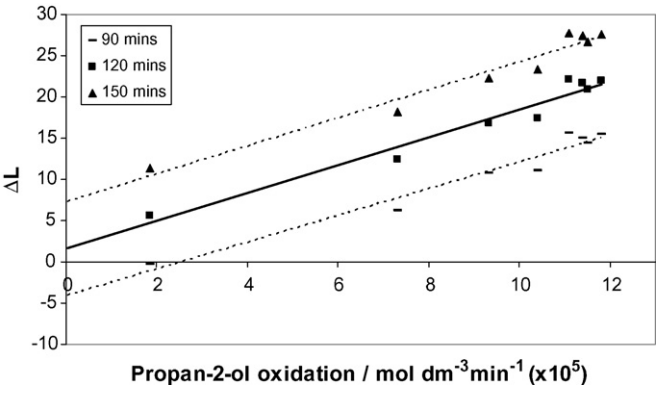

Fig. 7. Photogreying (for three different photogreying exposure times) vs. propanol oxidation rate. (The 90 and 150 min photogreying values have been arbitrarily displaced by 5 units to avoid overlap of the results.)

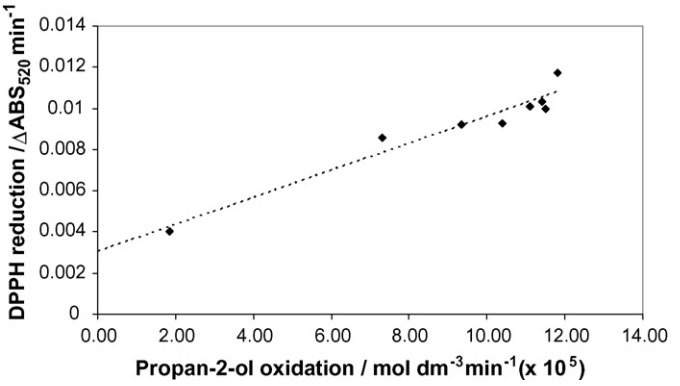

Fig. 8. Correlation of the DPPH$^{\bullet}$ photoreduction rate with the rate of photooxidation of propan-2-ol.

4. Discussion

4.1. Photoactivity dependence on coating level

For simplicity we assume that the TiO_2 crystals are spherical with a radius, r, given by $r = 3/A\rho_{TiO_2}$, where A is the specific surface area, measured by nitrogen adsorption, and ρ_{TiO_2} is the density of rutile. If we further assume that the silica is deposited as a uniform layer of thickness, t, and density ρ_{coat}, the weight

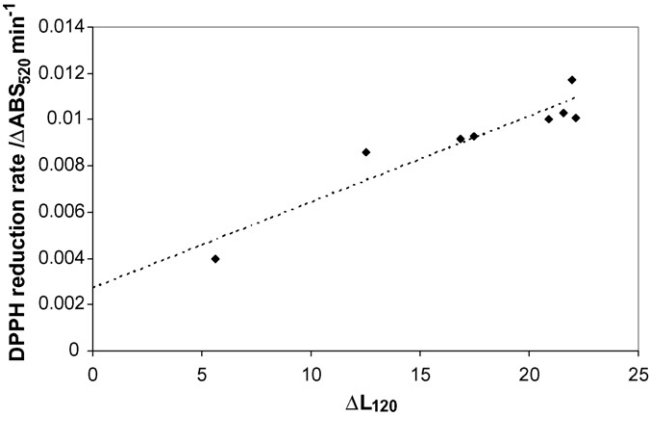

Fig. 9. Comparison of DPPH$^{\bullet}$ photoreduction rate and photogreying.

of coating is $W = 4\pi r^2 \rho_{coat} t$. The density of rutile is 4.26 g cm^{-3} and although we do not know exactly the density, ρ_{coat}, of the silica coating, an estimate of 2.13 g cm^{-3} [23] is convenient and reasonable. The weight of a rutile sphere is $4\pi r^2 \rho_{TiO_2}$ and if we assume a silica monolayer thickness of 0.5 nm, the amount calculated to cover the rutile surface is:

$$SiO_2\,(wt.\%) = \left[\frac{\text{weight of silica}}{\text{weight of } TiO_2}\right] \times 100$$

$$= \left[\frac{4\pi r^2 \rho_{coat} t}{(4/3)\pi r^3 \rho_{TiO_2}}\right] \times 100 = \left[\frac{3t\rho_{coat}}{r\rho_{TiO_2}}\right] \times 100$$

Substituting for ρ:

$$\text{silica}\,(wt.\%) = \frac{3t \times 0.5 \times 100}{r} = 15\%$$

which compares well with the three experimentally obtained values of 12 wt.% from propan-2-ol oxidation, 16 wt.% from DPPH photoreduction and 13 wt.% from photogreying. This suggests that the integrity of the coating is good and that the silica forms a reasonably uniform layer on the surface.

4.2. Correlation of photoreduction reactions with photooxidation

The good correlation, passing through the origin, shown in Fig. 7 between the measured photogreying and the rates of photooxidation is consistent with the earlier [22] hypothesis that photogeneration of charge carriers is the initial step in the oxidation of propanol and, in the absence of alternative electron acceptors, reduction of Ti^{4+} to Ti^{3+}. Fig. 8 demonstrates that there is also a good correlation between rates of DPPH reduction and propan-2-ol oxidation. However, for DPPH the best-fit line does not go through (or near) zero. The DPPH reduction rate corresponding to zero photooxidation is ~25% of the rate for uncoated rutile (or 15% if the comparison is based on first order kinetic plots for DPPH reduction—for which the R^2-values are less good) and this is larger than the 'dark' reaction contribution of ~5% reported above and shown in Fig. 4. The plot of DPPH reduction versus photogreying, Fig. 9 shows a similar non-zero intercept.

The difference in the intercepts is consistent with the hypothesis that in the absence of an electron acceptor, all unrecombined photogenerated electrons are captured by a Ti^{4+}, whereas in the presence of the DPPH some electrons may still be accepted by the Ti^{4+}. Consequently, reduction of DPPH by the uncoated rutile will be less than if all electrons are transferred. Thus, lowering of activity of the uncoated rutile would lower the gradient of the DPPH/propan-2-ol, or DPPH/photogreying line and result in a positive intercept on the DPPH axis.

4.3. A comparison of the absolute rates of photoreduction and photooxidation

Because of the need to obtain reproducible measurements of the DPPH bleaching, the study of DPPH reduction was carried out at lower catalyst loadings than were used for propan-2-ol oxidation. If no correction was made for catalyst loading, 80 propan-2-ol molecules were, on average, oxidised for each DPPH molecule reduced.

A comparison has been based on normalizing the rates to a catalyst loading of 1 g dm^{-3} (since doubling the TiO_2 loading increased DPPH reduction rate by 20% and propan-2-ol oxidation rate by 25% [24].) However, this normalization is crude, and, e.g., it ignores the effects of possible differences of catalyst dispersion on the optics of suspension. Nevertheless the estimate suggests that on average 2.5 molecules of propan-2-ol are oxidized for each DPPH reduced. This would be consistent with a mechanism by which each molecular radical of DPPH is reduced by one electron:

$$e^- + DPPH^\bullet \rightarrow DPPH^-$$

whereas each propan-2-ol may be oxidized both by a hydroxyl radical and by the less reactive perhydroxyl radical (proton transfer from water to $O_2^{\bullet -}$ is considered favourable to direct propan-2-ol oxidation by the oxygen radical due to the pK_a of water being lower than that of propan-2-ol) [25]:

$$h^+ + OH_{surf}{}^- \rightarrow OH^\bullet,$$

$$e^- + O_2 \rightarrow O_2^{\bullet -},$$

$$\text{followed by } O_2^{\bullet -} + H_2O \rightarrow HOO^\bullet + OH_{surf}{}^-$$

4.4. The dependence of the rates of photoreduction and photooxidation on the level of silica surface treatment

The dependence, shown in Fig. 10a, of photoreduction and photooxidation reaction rates on the level of silica coating suggests that the relationship is more complex than a simple 2.5:1 ratio (although this comparison is based on the normalized rates, the same activity pattern, though not the same ratio of rates, would be obtained for the non-normalized results). At low coating levels the ratio increases, reaching a maximum of 3:1 at 1 wt.% and then begins to decrease. By 10 wt.% the ratio is approaching 1:1. A possible explanation is that as the silica coating level increases from 0 to ~1 wt.%, the coating, which NMR shows to be not extensively cross-linked, preferentially blocks the transfer of electrons rather than holes. These blocked electrons could either recombine with a hole or become trapped by titanium atoms. Fig. 10b shows that at low loadings photogreying increases with respect to DPPH reduction, which is consistent with blocked electrons becoming trapped at Ti^{4+} sites and not recombining with holes. It has been shown previously [26,27] that Ti^{4+} sites involved in Ti–O–Si bonds have a greater electron affinity than those in Ti–O–Ti bonds which is in agreement with the changing ratios observed at low loadings. At higher levels of silica coating, corresponding to the increased cross-linking of silica shown by the NMR, transfer of holes is progressively blocked allowing the ratio to approach 1:1. Such differences could reflect either increased probability of cross-linking/condensation of silica at higher coverages or changes in silica location on the titania surface as the initial sites are occupied with increasing coverage. However, the above discussion is necessarily speculative and additional NMR studies to fur-

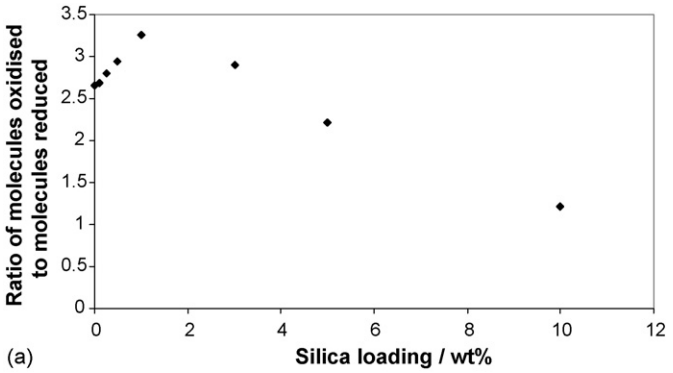

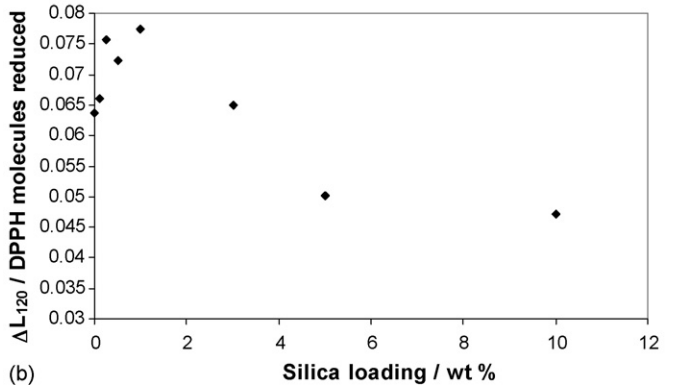

Fig. 10. (a) Variation in photooxidation:photoreduction ratio with silica content and (b) variation in photogreying:photoreduction reduction ratio with silica content. Photogreying values are as ΔL_{120} and photoreduction values are as molecules of DPPH$^{\bullet}$ reduced per minute per gram of catalyst.

ther test this speculation are in progress. Systematic trends such as those associated either with the differences in TiO_2 dispersion or with our normalisation procedure, might also account for differences in the estimated ratio.

Finally, if we compare the measured ΔL_{120} values with the DPPH reduction it can be seen that (under the experimental conditions used for photogreying) a value of one photogreying unit is equivalent to approximately 15×10^{16} DPPH molecules (per minute per gram of catalyst) being reduced. Correspondingly a ΔL value of one is equivalent to approximately 40×10^{16} propan-2-ol molecules being oxidised.

5. Conclusion

Our results demonstrate, to a first approximation, that on a series of treated rutile samples, photooxidation, as measured by propan-2-ol oxidation and photoreduction, parallels one another. For both reactions, the relationship between activity and silica coating level suggest that around 15 wt.% silica would be required to reduce the activity to effectively zero which is consistent with simple calculations. There is also an excellent correlation between photogreying and propan-2-ol oxidation. Based on a more detailed study of the effect of low levels of surface treatment, we speculate that at low silica levels electron transfer may be blocked more effectively than (direct or indirect) hole transfer.

Acknowledgements

We are grateful to Uniqema (Dr. I. Tooley) for financial support via an EPSRC CASE award (JAM), also for the provision of the high area rutile sample and many helpful discussions. We are grateful to Dr. David Apperley and the EPSRC solid-state NMR service for measuring the NMR spectra.

References

[1] F.S. Stone, An. Real. Soc. Espan Fis. Quim. B 61 (1965) 109.
[2] F.S. Stone, Ipatieff Centenary Symposium, Evanston, Illinois, U.S.A., 1967.
[3] R. Rudham, R.B. Cundall, M.S. Salim, J. Chem. Soc., Faraday Trans. 1 (72) (1976) 1642–1651.
[4] R. Rudham, P.R. Harvey, S. Ward, J. Chem. Soc., Faraday Trans. 1 (79) (1983) 1381–1390.
[5] G. Irick, J. Appl. Polym. Sci. 16 (1972) 2387.
[6] A.E. Regazzoni, P. Mandelbaum, M. Matsuyoshi, S. Schiller, S. Bilmes, M.A. Blesa, Langmuir 14 (1998) 868–874.
[7] D.W. Bahnemann, S.N. Kholuiskaya, R. Dillert, A.I. Kulak, A.I. Kokorin, Appl. Catal. B: Environ. 36 (2002) 161–169.
[8] A. Horvath, H. Czili, E. Szabo-Bardos, J. Photochem. Photobiol. A: Chem. 154 (2003) 195–201.
[9] X. Domenech, J. Peral, J. Ayllon, M. Franch, Catal. Today 76 (2002) 221–233.
[10] T.A. Egerton, P.A. Christensen, R.W. Harrison, J.W. Wang, J. Appl. Electrochem. 35 (2005) 799–813.
[11] M.R. Hoffmann, L. Bourne, N.J. Peill, J. Photochem. Photobiol. A: Chem. 108 (1997) 221–228.
[12] A. Heller, Y. Degani, D.W. Johnson, P.K. Gallagher, J. Phys. Chem. 91 (1987) 5987–5991.
[13] T.A. Egerton, I.R. Tooley, Conference Proceedings, Photocatalytic and Advanced Oxidation Processes for Treatment of Air Water Soil and Surfaces, 2004, pp. 95–101.
[14] M.R. Hoffmann, W. Choi, Environ. Sci. Technol. 29 (1995) 1646–1654.
[15] M.R. Hoffmann, W. Choi, J. Phys. Chem. 100 (1996) 2161–2169.
[16] E. Pelizzetti, C. Minero, P. Calza, J. Chem. Soc., Faraday Trans. 93 (1997) 3765–3771.
[17] T.G. Truscott, D.J. McGarvey, P.L. Lyth, P.J. Guest, G. Dransfield, J. Photochem. Photobiol. B: Biol. 59 (2000) 151–174.
[18] G. Wakefield, S. Lipscomb, E. Holland, J. Knowland, Photochem. Photobiol. Sci. 3 (2004) 648–652.
[19] R.K. Iler, US Patent No. 2,885,366 (1959), to E.I. du Pont de Numours.
[20] G. Engelhardt, D. Michel, High-resolution Solid-state NMR of Silicates and Zeolites, 1st ed., Wiley, 1987.
[21] T.A. Egerton, I.R. Tooley, J. Mater. Chem. 12 (2002) 1111–1117.
[22] T.A. Egerton, I.R. Tooley, L.M. Kessell, L. Wang, J. Nanoparticle Research (NANO0622), submitted for publication.
[23] J.D. Willey, Kirk Othmer Encyclopedia of Chemical Technology, vol. 20, 3rd ed., John Wiley & Sons Inc., New York, 1982, p. 766.
[24] I.R. Tooley, Ph.D. Thesis, University of Newcastle Upon Tyne, 2001.
[25] R.B. Cundall, R. Rudham, M.S. Salim, J. Chem. Soc., Faraday Trans. 72 (1976) 1642–1651.
[26] J.T. Yates Jr., D. Panayotov, Chem. Phys. Lett. 381 (2003) 154–162.
[27] I.E. Wachs, X. Gao, Catal. Today 51 (1999) 233–254.